

Synthesis of glycine-containing complexes in impacts of comets on early Earth

Nir Goldman^{*}, Evan J. Reed[†], Laurence E. Fried, I.-F. William Kuo and Amitesh Maiti

Delivery of prebiotic compounds to early Earth from an impacting comet is thought to be an unlikely mechanism for the origins of life because of unfavourable chemical conditions on the planet and the high heat from impact. In contrast, we find that impact-induced shock compression of cometary ices followed by expansion to ambient conditions can produce complexes that resemble the amino acid glycine. Our *ab initio* molecular dynamics simulations show that shock waves drive the synthesis of transient C-N bonded oligomers at extreme pressures and temperatures. On post impact quenching to lower pressures, the oligomers break apart to form a metastable glycine-containing complex. We show that impact from cometary ice could possibly yield amino acids by a synthetic route independent of the pre-existing atmospheric conditions and materials on the planet.

Origins-of-life research focused initially on the production of amino acids from organic materials already present on the planet. In addition to protein production, amino acids and short peptides probably played a significant role in the chemical evolution that led to the emergence of life¹. Peptide nucleic acids, which consist of a backbone of achiral poly(*N*-(2-aminoethyl)glycine), were proposed as a precursor to ribonucleic acid (RNA) on early Earth². Polypeptides were shown to catalyse the formation of RNA in an energetically favoured reaction in which activated mononucleotides were used³. Seminal experiments^{4,5} observed amino-acid synthesis in a vaporized reducing (H₂- and CH₄-rich) mixture subjected to electrical discharges to simulate hypothetical conditions on the early planet. However, the actual composition of early Earth's atmosphere is not known, and the current view is that the atmospheric conditions were more oxidizing¹, consisting mainly of CO₂, N₂ and H₂O, with only small amounts of CO and H₂. Shock-heating experiments^{6,7} and calculations⁸ on aqueous mixtures found that synthesis of the organic molecules necessary for amino-acid production does not occur in a CO₂-rich environment.

The possibility exists of the production and/or delivery of prebiotic molecules from extraterrestrial sources. Cometary ices are predominantly water^{9,10}, but contain many small molecules important to prebiotic aqueous chemistry, such as CO₂, NH₃ and CH₃OH (ref. 9). Recent analysis of dust samples from comet Wild 2 showed the presence of glycine in the captured material¹¹. Interplanetary dust particles accrete icy layers that consist of H₂O, CO, CO₂, CH₃OH and NH₃ (ref. 12). The flux of organic matter to Earth from comets and asteroids during periods of heavy bombardment may have been as high as 10¹³ kg yr⁻¹, delivering up to several orders of magnitude greater mass of organics than probably pre-existed on the planet¹³.

The median nucleus radius of short-period comets was measured as 1.61 km, and long-period comets can have nucleus radii up to 56 km (ref. 14). A comet of such sizes that passes through Earth's atmosphere will be heated externally, but will remain cool internally. On impacting the planetary surface, a shock wave will be generated because of the sudden compression. The shock wave travelling through the comet will compress a small section of material on a timescale limited by the rise time of the shock wave (<10 ps)¹⁵⁻¹⁷.

A shock wave causes a reactive material to visit numerous thermodynamic states during the course of compression. Shock waves can create sudden, intense pressures and temperatures, which could affect chemical pathways and reactions within a comet before interactions with the ambient planetary atmosphere can occur. Until now, the overall delivery and/or production of amino acids from these impact events was thought to be improbable because of the extensive heating (thousands of K) from the impact, which would cause pyrolysis of organic compounds¹⁸. However, an oblique collision in which an extraterrestrial ice impacts a planetary atmosphere with a glancing blow would generate much lower temperatures¹³. Shock compression followed by a rarefaction wave and subsequent expansion would occur over the course of several seconds¹⁹. Under this scenario, organic materials could potentially be synthesized within the interior of the comet during shock compression and survive the high pressures and temperatures. On expansion, stable materials, such as amino acids, could survive interactions with the planetary atmosphere or ocean. These processes would result in large concentrations of organic species being delivered to Earth from exogenous sources. Shock-compression experiments on cometary mixtures showed that a high percentage of pre-existing amino acids survived relatively low pressure conditions (412–870 K and 5–21 GPa; 1 GPa = 10 kbar)¹³ and that mixtures resembling carbonaceous chondrites can produce a variety of organic material at pressures of ~6 GPa (ref. 20). The production of amino acids by ultraviolet irradiation of interplanetary dust particles^{12,21} and amino-acid condensation in the presence of a catalyst²² were investigated. Hydrodynamic simulations of large cometary impacts indicated the release of large quantities of gas by carbonaceous rock¹⁹. Nonetheless, to date few studies are reported on the production of prebiotic molecules at both the extreme temperatures and pressures (for example, >1,000 K and 20 GPa) that result from the impact of a large icy body such as a comet.

Molecular dynamics (MD) simulations provide an accurate description of shock compression, which can greatly facilitate experimental design and interpretation. Simulating the breaking and forming of chemical bonds behind a shock front frequently requires the use of a quantum theory such as density functional theory (DFT);

Physical and Life Sciences Directorate, Chemical Sciences Division, Lawrence Livermore National Laboratory, Livermore, California 94550, USA; [†]Present address: Department of Materials Science and Engineering, Stanford University, Stanford, California 94304, USA. *e-mail: goldman14@llnl.gov

for example, see Gygi and Galli²³). DFT has been shown to reproduce accurately the high pressure–temperature properties of a number of systems, including deuterium²³, nitrogen²⁴, carbon²⁵ and the solid and liquid phases of water^{26–28}. Here, we report DFT–MD simulations of amino-acid synthesis in a shock-compressed prototypical astrophysical ice mixture. DFT–MD simulations can access readily the picosecond timescales associated with the rise time of a shock wave^{25,28}. To perform simulations of the unique thermodynamic conditions of a shock^{25,29} and minimize the usual system-size issues¹⁷, we used the multiscale shock-compression simulation technique (MSST)^{29–31}. MSST allows for an approximate treatment of the hydrodynamic effects in cometary impact, combined with a realistic description of the chemistry at extreme conditions. MSST is a simulation methodology based on MD and the Navier–Stokes equations for compressible flow. Instead of simulating a planar shock wave within a large computational cell with many atoms, the MSST computational cell follows a Lagrangian point through the shock wave. MSST does not include non-planar shock waveforms. MSST was shown to reproduce accurately the shock Hugoniot (thermodynamic end states) of a number of systems^{25,28}, as well as the sequence of thermodynamic states throughout the reaction zone of shock-compressed explosives³¹. MSST can reproduce the same shock-wave profiles, physics and chemistry as found in direct, multi-million particle simulation of shock compression³² (see Supplementary Information for more details).

Amino acids contain both amine ($-\text{NH}_2$) and carboxyl ($-\text{COOH}$) functional groups, and require the formation of C–N bonds for their synthesis. Protein synthesis is driven by peptide bond formation, that is C–N bonds formed between $-\text{COOH}$ and $-\text{NH}_2$ groups from different amino acids with an H_2O group eliminated. Hence, our goal is to create a more fundamental understanding of C–N bond formation and the survivability of such species as a function of elevated temperatures and pressures caused by shock compression. Similar to previous experiments¹², our studies contained a mixture of H_2O , CH_3OH , NH_3 , CO and CO_2 in a molar ratio of 2:1:1:1:1, respectively. Our simulations (706–4,083 K, 10–59 GPa) far exceeded the pressure–temperature ranges of previous shock-compression studies^{13,20}. Simulations at higher temperatures and pressures resulted in excitations beyond the electronic ground state, similar to those of a plasma. Our computed shock Hugoniot results show correspondence with previous experimental^{33,34} and theoretical²⁸ results for liquid water (see Supplementary Information). Astrophysical ice with an initial velocity of 29 km s^{-1} (approximate median encounter velocity of a short-period comet with Earth¹³) would have to impact the Earth at an angle from the horizontal of up to 24° to experience the pressures and temperatures of our simulations. Assuming a probability distribution of $dP = \sin(2\phi)d\phi$, where ϕ is the angle from the horizon³⁵, our simulations correspond to low-velocity impacts with a cumulative 17% probability (Fig. 1). Thus, our study encompasses probable events for astrophysical ice impacts on early Earth.

Results and discussion

A constant-pressure state was achieved within 0.4–3.0 ps in all shock-compression simulations. The time over which cometary ice of radius 1.61 km would be held in this hot, compressed state before the arrival of a rarefaction wave and subsequent decompression is approximately 0.4 seconds (see Supplementary Information). However, previous results show the rise time of the shock wave (the viscosity-induced width of the shock front) in polycrystalline materials to be <10 ps (refs 15,16). Shock-compression studies of materials with micrometre-sized grains (similar to grain sizes found in comets³⁶) found sharply focused shock waves that traversed across each individual grain³⁷. Our shock-compression

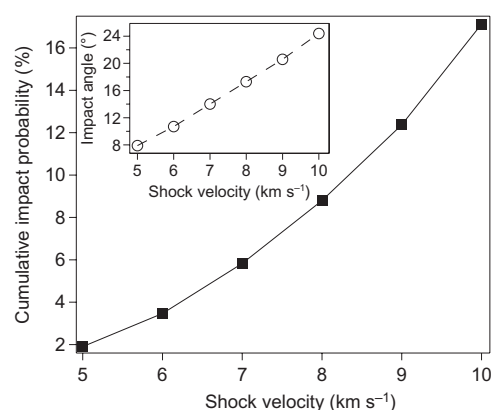


Figure 1 | The cumulative probability of impact for our simulated shock velocities. The computed probability corresponds to the chance of impact from zero up to a given particle velocity, which is related to the shock velocity as shown in the Methods section. A comet that travels at a velocity of 29 km s^{-1} would have to impact a planet at an angle of 8° to achieve a shock velocity of 5 km s^{-1} , and at 24° for 10 km s^{-1} . For a shock velocity of 10 km s^{-1} , the impact angle distribution model of Shoemaker³⁵ gives a cumulative probability of 17%. Shock velocities from previous studies^{13,20} correspond to probabilities of impact of about 0.5% and 2%, respectively. Inset: computed impact angles for our simulated shock velocities.

simulations (up to 11 ps in length) thus span the relevant timescales that correspond to the initial chemistry behind the shock wave within an ice grain in a comet. These timescales are amenable to study by laser shock-compression experiments¹⁶.

After compression, our simulations formed a series of new compounds (Fig. 2). At 47 GPa (shock velocity of 9 km s^{-1} , Hugoniot temperature of 3,141 K) almost none of the starting materials remained, aside from small mole fractions of H_2O and NH_3 . We observed a number of complex C–N bonded species and H^+ ions. Our results showed that the C–N bond kinetics achieved a steady state after several picoseconds (see Supplementary Information). The quantity and complexity of C–N bonded species grew rapidly as a function of pressure. We have analysed the chemical species prevalent in the shock-compressed astrophysical ice at these conditions.

We defined molecular species using a pre-established methodology of optimal bond cutoff distances and lifetimes^{38–40}. At 10 GPa (5 km s^{-1} , 706 K) we observed the formation of NH_2COO^- (namely, carbamate, the simplest molecule that contains both amine and carboxyl groups). The carbamate anion (unstable under ambient aqueous conditions) formed within 2 ps of shock compression, and survived through the remainder of the simulation. On achieving a steady pressure state, approximately 76% of the starting material remained, and the lifetime of H_2O was calculated as 1.65 ps, many orders of magnitude shorter than its lifetime at ambient conditions (~ 10 hours⁴¹). Water at extreme conditions was shown to catalyse chemical reactivity in C–N–O–H materials⁴². At 24 GPa (7 km s^{-1} , 1,590 K), we observed that 53% of the starting material remained, and that the H_2O lifetime decreased to 360 fs. Thus, we expected a high degree of chemical reactivity at these conditions. At this pressure and temperature we observed a mole fraction of 0.05 for many different C–N bonded species with lifetimes between 65 and 120 fs, and an additional mole fraction of 0.03 for C–N bonded species with lifetimes <50 fs. In addition, we calculated an H^+ mole fraction of 0.11. The free hydrogen ions created a localized reducing environment that could drive C–N bond formation in otherwise oxidizing conditions. Shock compression to 47 GPa (9 km s^{-1} , 3,141 K) and 59 GPa (10 km s^{-1} , 4,083 K) both yielded a similarly high degree

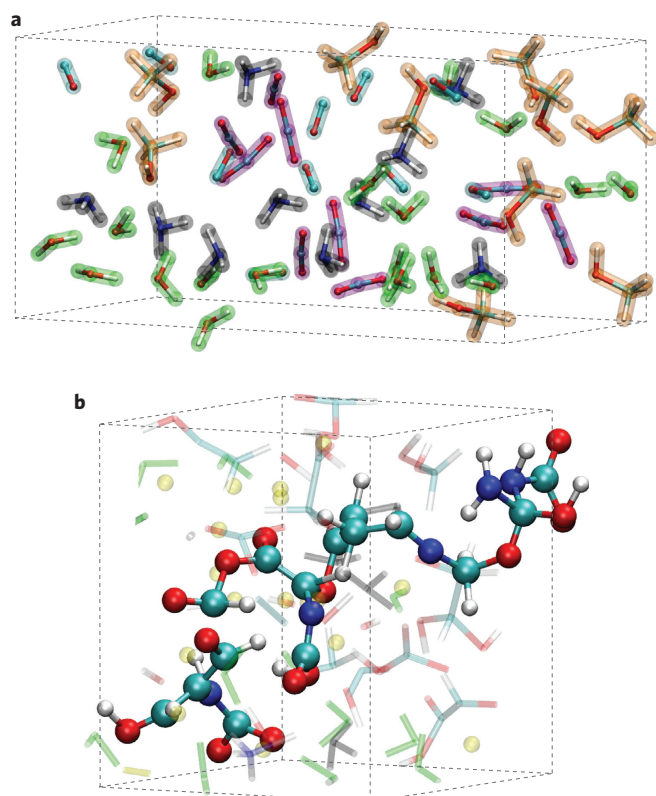


Figure 2 | Snapshots of the computational cell. a, b At the initial conditions (**a**) and during shock compression at 9 km s^{-1} (47 GPa) (**b**). For all of our simulation snapshots, H_2O molecules are coloured green, NH_3 black, CO light blue, CO_2 purple and CH_3OH orange. For the atoms, oxygen is red, hydrogen is white, carbon is light blue and nitrogen is dark blue. In (**b**) the smaller size of the simulation cell results from the shock compression. For clarity we show only atomic sites for C–N bonded species (opaque) formed during shock compression. All other species (transparent) are shown by their bonds only, excluding H^+ ions, which are shown as yellow spheres. After shock compression, all of the CH_3OH and CO_2 are consumed. A small number of H_2O and NH_3 molecules are still observed, as well as a single CO molecule. Shock compression caused several exotic species to form, including the large carbon chain-like oligomer with several C–N bonds shown in the middle of the snapshot.

of chemical reactivity and molecular ionization throughout the simulations. We discuss the trajectory at 47 GPa in detail here.

At 47 GPa, the highly transient nature of covalent bonding in the hot, compressed system produced a large number of short-lived species, which yielded a computed mole fraction of C–N bonded species of 0.03. The atomic fraction of C–N bonded species (number of atoms in C–N bonded species divided by the total number of atoms in the simulation) was approximately 24%. The mole fraction of H^+ increased to 0.35. Only 16% of the starting material remained, and the H_2O lifetime decreased to $<80 \text{ fs}$. At this point it became difficult to describe the system as having molecular species because the calculated lifetimes were all roughly equal to the chosen cutoff. Under these extreme conditions, we observed a large number of exotic C–N bonded species (Fig. 3a). NH_2COO^- was observed to react with organics such as HCOOH to form larger, transient species. Some species showed the formation of C–C bond chains by reactions with CO_2 and HCO^- moieties, indicative of a mechanism that could form complex amino acids.

To approximate the expansion that occurs immediately after planetary impact and shock compression, we expanded the system from 47 GPa in discrete constant pressure–temperature (NPT)

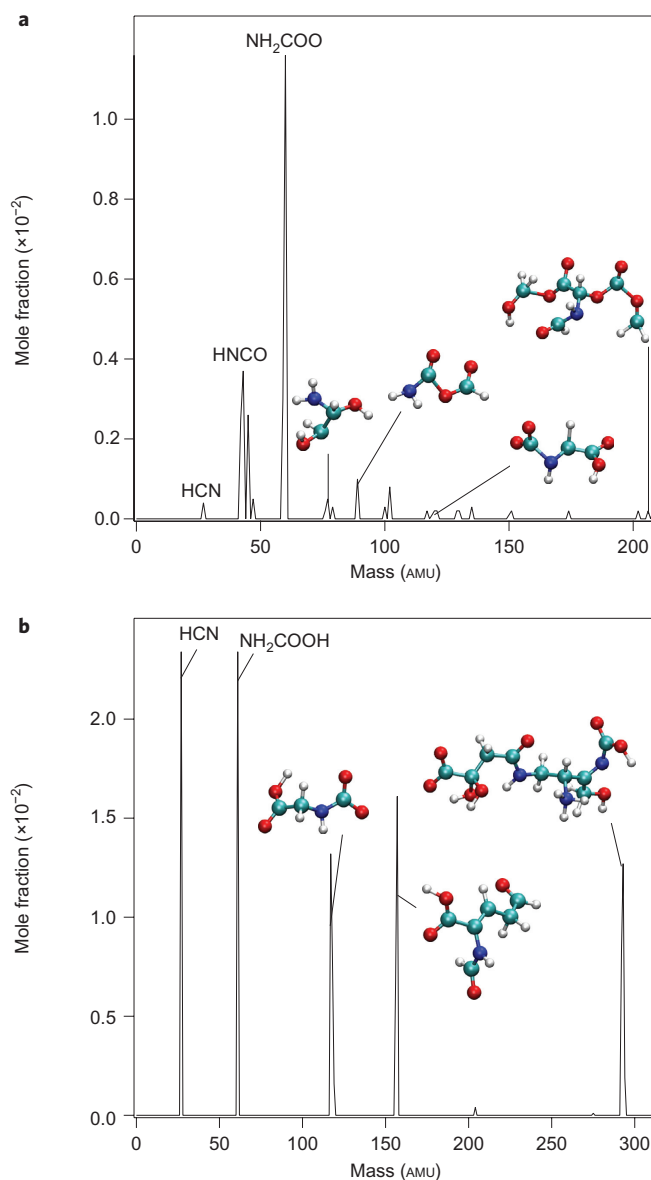


Figure 3 | Simulated mass spectra of the C–N bonded molecules found during our simulations. a, During shock compression to 47 GPa (9 km s^{-1}). Chemical formulae are provided for selected peaks, and graphics are shown for the more exotic species. At 47 GPa, numerous C–N oligomers with mass peaks over 300 AMU had lifetimes less than our lifetime criterion (50 fs) and are not included in the plot. **b**, After quenching both temperature and pressure, we observed significant quantities of a glycine– CO_2 complex at a mass peak of 118 AMU.

steps along the water isentrope. Each step was between 2 and 4 ps in duration, for a total expansion simulation time between 15 and 28 ps. The water isentrope was computed from a recent equation of state⁴³ (see Supplementary Information). Cometary ice with a radius of 1.61 km and a speed of sound similar to that of water (1.482 km s^{-1} at 20°C) takes over two seconds to expand. It is not possible to model this timescale by MD simulation. However, the expanding comet visits approximately the same locus of thermodynamic states as our expansion simulations. Calculations have shown that the chemical reactions within expanding cometary materials quench at temperatures between 2,000 and 3,000 K (ref. 7). After expanding to a pressure of 0.5 GPa and a temperature of 1,550 K, the system remained largely unreactive on the timescales

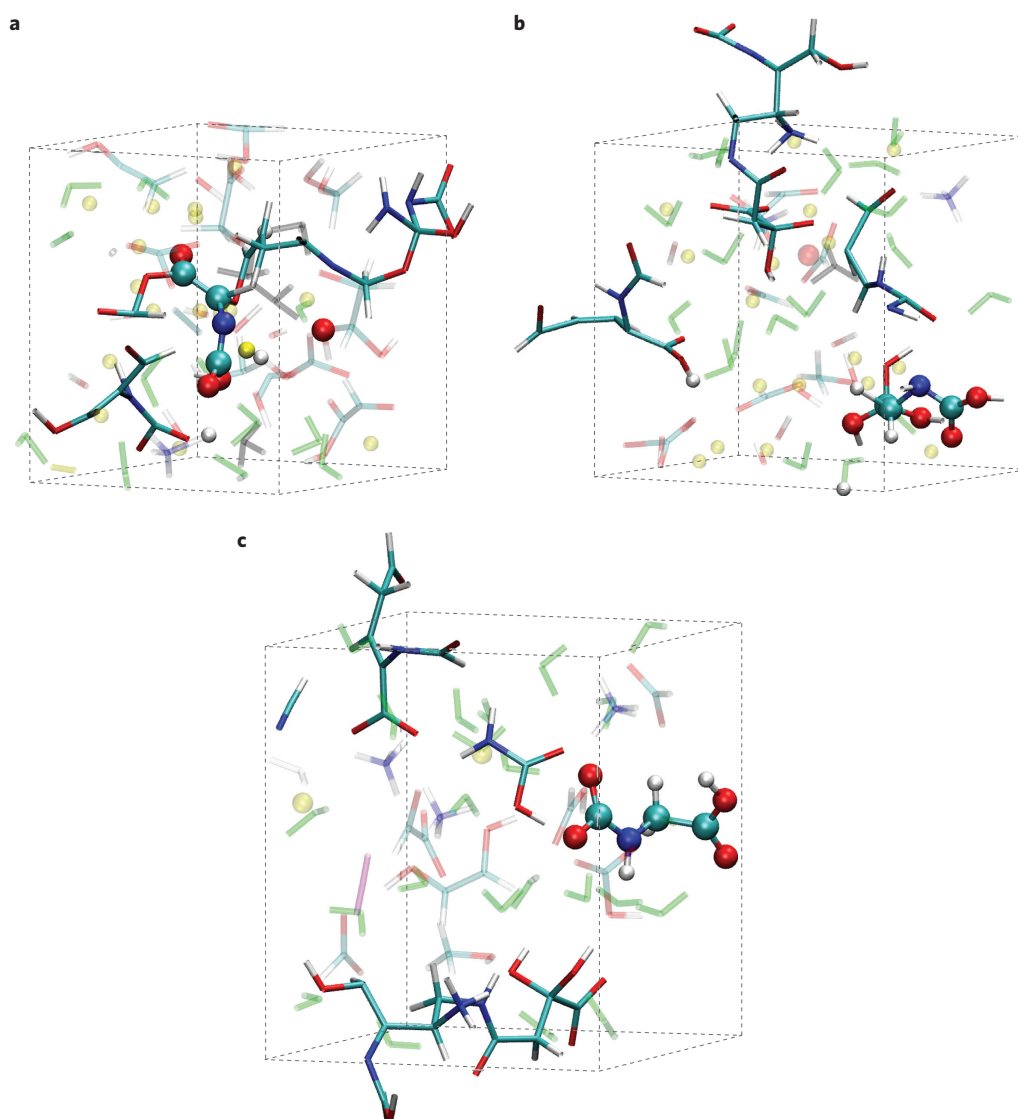


Figure 4 | Mechanism for glycine- CO_2 complex synthesis on expansion and cooling. **a**, The high pressures and temperatures from shock compression (47 GPa (9 km s^{-1})) caused a large C–N bonded oligomer to form. In this species, we observed a sequence of carbon and nitrogen atoms that corresponded to that of glycine (only the atomic sites that eventually form the complex $^- \text{OCO-NH-CH}_2\text{-COOH}$ are shown here and in **(b)** and **(c)**). **b**, During isentropic expansion (16.6 GPa , $2,673 \text{ K}$), the large C–N bonded chain in **(a)** broke apart to form several fragments. The C–N sequence that corresponds to glycine remained intact during the expansion. A significant quantity of H^+ ions remained in the system, although we also observed an increase in the number of H_2O molecules. **c**, On cooling to the initial conditions (0.5 GPa , 300 K), we observed the formation of several stable and metastable C–N bonded species, including HCN , $\text{NH}_2\text{-COOH}$ and a more complex molecule with several C–N bonds. A single CO_2 molecule was observed also. Smaller moieties, such as H and OH , are eliminated from the C–N backbone that forms $^- \text{OCO-NH-CH}_2\text{-COOH}$. This species can react with a proton source, such as H_3O^+ , to form glycine.

of our simulations. Longer timescale effects of elevated post shock temperatures on chemical products are the subject of future work. Further expansion along the isentrope would yield a low-density gas, which would be difficult to simulate with our planewave-based DFT method. To test the stability of compounds formed during our simulations, we quenched the system temperature in three sequential steps to 300 K . After expanding the simulation cell, NPT simulations were run at 300 K for an additional $10\text{--}20 \text{ ps}$. The longest of our simulations of the adiabatic expansion covered approximately 50 ps in total. A single expansion–cooling cycle required $\sim 80,000$ central processing unit hours, which limited the rate at which the cycle could be performed. Determination of the chemistry after adiabatic expansion as the material interacts with the planetary environment was beyond the scope of this study.

Several quenches were performed with varying numbers of NPT steps and at different points in time along the shock-compressed trajectory, all of which exhibited the survival of several stable C–N bonded species (Fig. 3b). In particular, we observed consistently a synthetic route to complexes that resembled the amino acid glycine through the decomposition of large C–N bonded oligomers. Glycine is the simplest proteinogenic amino acid and has a chemical formula of $\text{NH}_2\text{CH}_2\text{COOH}$. We observed a possible mechanism for its ‘shock synthesis’ which began with the formation of its C–N backbone during shock compression (Fig. 4a). The high pressures and temperatures allowed for the rapid formation of the C–N bonded oligomers, which contain sequences of carbon and nitrogen atoms that resemble those of several amino acids. Isentropic expansion caused the oligomer to break apart into smaller fragments (Fig. 4b). These fragments were highly reactive and had lifetimes between 50 and

200 fs, although their C–N backbone could remain intact. Cooling then caused the fragments to eliminate smaller moieties (for example, OH and H) to form species such as the anion $^{-}\text{OCO-NH-CH}_2\text{-COOH}$ (Fig. 4c). This glycine-CO₂ complex requires a one-step protonation reaction to form glycine. We computed significant mole fractions of H₃O⁺ (0.03) and NH₄⁺ (0.07) in our cooled and expanded simulations. Calculations with a quantum-chemical solvation model⁴⁴ showed that protonation of $^{-}\text{OCO-NH-CH}_2\text{-COOH}$ either by H₃O⁺ or NH₄⁺ in a solvent environment representative of our quenched and cooled simulations was thermodynamically favourable. The glycine-formation reaction of $^{-}\text{OCO-NH-CH}_2\text{-COOH} + \text{H}_3\text{O}^+ \leftrightarrow \text{CO}_2 + \text{H}_2\text{O} + \text{NH}_2\text{-CH}_2\text{-COOH}$ has a Gibbs free energy of reaction (ΔG_{rxn}) of $-24.2 \text{ kcal mol}^{-1}$. The reaction of $^{-}\text{OCO-NH-CH}_2\text{-COOH} + \text{NH}_4^+ \leftrightarrow \text{CO}_2 + \text{NH}_3 + \text{NH}_2\text{-CH}_2\text{-COOH}$ has a ΔG_{rxn} of $-2.2 \text{ kcal mol}^{-1}$ (see Supplementary Information for more details). Thus, the complex C–N bonded oligomers could form glycine given realistic timescales of the isentropic expansion after an impact event. Also, frequently we observed in our quenched simulations mole fractions up to 0.03 of HCN and 0.07 of formic acid (HCOOH). HCN and formaldehyde (H₂CO) are known to be precursors for amino acid and complex organic synthesis^{7,8,21}. One of our quenches produced a mole fraction of 0.02 of NH₂-(CH₂)₂-COOH, which indicates the possibility of creating amino acids with greater complexity through the shock-synthesis mechanism.

Conclusions

Our simulations provide a possible mechanism for the ‘shock synthesis’ of prebiotic molecules on early Earth that is independent of the atmospheric conditions and materials already present on the primitive planet. Novel experiments capable of monitoring complex time-dependent chemical reactivity in shock-compressed systems⁴⁵ hold promise to verify this synthetic route. On shock compression, we observed a high degree of chemical reactivity at extreme conditions, with large concentrations of H⁺ ions, which create local reducing environments. This reactive environment helps induce the formation of C–N bonded oligomers that contain sequences of C–N bonds equivalent to those of alpha amino acids. On quenching to lower pressures and temperatures, the oligomers break apart to form more stable complexes. Many of these complexes can react easily with H⁺ to form glycine. Other exotic, metastable C–N species that we observed in our quenched simulations could conceivably form more complex amino acids or even peptide chains that resemble the proteins needed for the formation of life.

Methods

DFT-MD simulations. All simulations were performed with the CP2K molecular simulation software suite⁴⁶, using the Born–Oppenheimer approximation to maintain the system in its electronic ground state. Interatomic potentials were thus calculated on the fly from directly solving the Schrödinger equation. We used a plane-wave cutoff of 400 Ry and an optimized double zeta valence polarized basis set for all elements in the system. We employed Goedecker–Teter–Hutter pseudopotentials⁴⁷ with the Becke–Lee–Yang–Parr exchange correlation functional^{48,49}. We performed simulations at shock velocities (km s⁻¹) 5, 6, 7, 8, 9 and 10. Simulations were 5–11 ps in length, excluding the 10 km s⁻¹ shock compression, which was simulated only for 2 ps. For all of our simulations, we used an initial astrophysical ice configuration of twenty H₂O, ten CH₃OH, ten NH₃, ten CO and ten CO₂ molecules (210 atoms in total), with computational cell-lattice vectors of $\mathbf{a} = 21.915 \text{ \AA}$, $\mathbf{b} = 10.9575 \text{ \AA}$ and $\mathbf{c} = 10.9575 \text{ \AA}$. These cell dimensions yielded a density of 1.0 g ml⁻¹, similar to the initial conditions of the experiments¹². The initial temperature was set to 300 K. MD simulations were conducted with a time step of 0.1 fs. We used a fictitious box mass of $3.5 \times 10^6 \text{ AMU}$ and a wavefunction convergence criterion of 10^{-6} AMU for the shock-compression simulations. The initial configuration was equilibrated at 300 K for several picoseconds before the shock-compression simulation was conducted. Uniaxial compression of the shock wave occurred along the \mathbf{a} lattice vector. Charges can be associated with different species; we found that these varied according to the thermodynamic and chemical conditions present in the simulation cell²⁸.

Angle of impact. The particle velocity U_p of a shock-compressed system is related to the shock velocity U_s according to the relation $U_p = U_s(1 - \rho_0/\rho)$, where ρ_0 and ρ are

the initial and final densities, respectively⁵⁰. U_p from our simulations was related to the angle from the horizon ϕ according to the formula $U_p = (V_E/2)\sin \phi$. Here, V_E is the encounter velocity of the impacting extraterrestrial icy object. Impact with an ocean or other body with similar shock impedance to the extraterrestrial ice contributes an approximate factor of 1/2 because of the body’s compressibility.

Post simulation analysis. Similar to previous work^{38–40}, in our simulations we defined molecular species by first choosing an optimal bonding cutoff r_c for all possible bonds. The optimal value for r_c to distinguish between bonded and non-bonded atomic sites is given by the first minimum in the corresponding pair radial distribution function $g(R)$, which corresponds to the maximum of the potential of mean force, namely $W(R) = -k_B T \ln(g(R))$, for all possible bonding pairs. This choice corresponds to the optimal definition of the transition state within transition-state theory³⁸. In addition, to avoid counting species that were entirely transient and not chemically bonded³⁹, we also chose a lifetime cutoff of 50 fs. This criterion was intuitive because bonds with this lifetime could conceivably be detected spectroscopically. As a result, atom pairs were considered to be bonded only if they resided within a distance of each other of r_c for a time $>50 \text{ fs}$. Using these bonding criteria, specific molecular species were then defined by recursively creating a data tree of all atomic bonds that branched from the original bonded pair. The chemical reactivity, concentrations and lifetimes of different species were then determined by monitoring the creation and dissociation of specific molecules during the course of the simulations. Shorter and longer bond-lifetime criteria were also tested. We found that the computed species at quenched conditions and the overall conclusions of this work were independent of the choice of bond and lifetime criteria. The concentrations of species at high pressure and temperature have some dependence on bond and lifetime criteria, as expected and as shown for other hot, dense materials^{28,38}.

Received 30 March 2010; accepted 27 July 2010;
published online 12 September 2010

References

- Brack, A. From interstellar amino acids to prebiotic catalytic peptides: a review. *Chem. Biodiv.* **4**, 665–679 (2007).
- Nelson, K. E., Levy, M. & Miller, S. L. Peptide nucleic acids rather than RNA may have been the first genetic molecule. *Proc. Natl Acad. Sci. USA* **97**, 3868–3871 (2000).
- Barbier, B., Visscher, J. & Schwartz, A. W. Polypeptide-assisted oligomerization of analogs in dilute aqueous solution. *J. Mol. Evol.* **37**, 554–558 (1993).
- Miller, S. L. A production of amino acids under possible primitive earth conditions. *Science* **117**, 528–529 (1953).
- Miller, S. L. & Urey, H. C. Organic compound synthesis on the primitive earth. *Science* **130**, 245–251 (1959).
- Bar-Nun, A., Bar-Nun, N., Bauer, S. H. & Sagan, C. Shock synthesis of amino acids in simulated primitive environments. *Science* **168**, 470–473 (1970).
- McKay, C. P. & Borucki, W. J. Organic synthesis in experimental impact shocks. *Science* **276**, 390–392 (1997).
- Fegley, B. Jr, Prinn, R. G., Hartman, H. & Watkins, G. H. Chemical effects of large impacts on the Earth’s primitive atmosphere. *Nature* **319**, 305–308 (1986).
- Ehrenfreund, P. & Charnley, S. B. Organic molecules in the interstellar medium, comets, and meteorites: a voyage from dark clouds to the early earth. *Annu. Rev. Astron. Astrophys.* **38**, 427–483 (2000).
- Ehrenfreund, P. *et al.* Astrophysical and astrochemical insights into the origin of life. *Rep. Prog. Phys.* **65**, 1427–1487 (2002).
- Elsila, J. E., Glavin, D. P. & Dworkin, J. P. Cometary glycine detected in samples returned by stardust. *Meteorit. Planet. Sci.* **44**, 1323–1330 (2009).
- Muñoz Caro, G. M. M. *et al.* Amino acids from ultraviolet irradiation of interstellar ice analogues. *Nature* **416**, 403–406 (2002).
- Blank, J. G., Miller, G. H., Ahrens, M. J. & Winans, R. E. Experimental shock chemistry of aqueous amino acid solutions and the cometary delivery of prebiotic compounds. *Origins Life Evol. B* **31**, 15–51 (2001).
- Meech, K. J., Hainaut, O. R. & Marsden, B. G. Comet nucleus size distributions from HST and Keck telescopes. *Icarus* **170**, 463–491 (2004).
- Robertson, D. H., Brenner, D. W. & White, C. T. Split shock wave from molecular dynamics. *Phys. Rev. Lett.* **67**, 3132–3135 (1991).
- Gahagan, K. T., Moore, D. S., Funk, D. J., Rabie, R. L. & Buelow, S. J. Measurement of shock wave rise times in metal thin films. *Phys. Rev. Lett.* **85**, 3205–3208 (2000).
- Kadau, K., Germann, T. C., Lomdhal, P. S. & Holian, B. L. Microscopic view of structural phase transitions induced by shock waves. *Science* **296**, 1681–1684 (2002).
- Chyba, C. F., Thomas, P. J., Brookshaw, L. & Sagan, C. Cometary delivery of organic molecules to early earth. *Science* **249**, 366–373 (1990).
- Pierazzo, E., Kring, D. A. & Melosh, H. J. Hydrocode simulation of the Chicxulub impact event and the production of climatically active gases. *J. Geophys. Res.* **103**, 28607–28625 (1998).
- Furukawa, Y., Sekine, T., Oba, M., Kakegawa, T. & Nakazawa, H. Biomolecule formation by oceanic impacts on early Earth. *Nature Geosci.* **2**, 62–66 (2009).

21. Bernstein, M. P., Dworkin, J. P., Sandford, S. A., Cooper, G. W. & Allamandola, L. J. Racemic amino acids from the ultraviolet photolysis of interstellar ice analogues. *Nature* **416**, 401–403 (2002).
22. Huber, C. & Wächterhäuser, G. Peptides by activation of amino acids with CO on (Ni,Fe)S surfaces: implications for the origin of life. *Science* **281**, 670–672 (1998).
23. Gygi, F. & Galli, G. Electronic excitations and the compressibility of deuterium. *Phys. Rev. B* **65**, 220102 (2002).
24. Kress, J. D., Mazeret, S., Collins, L. A. & Wood, W. W. Density-functional calculation of the Hugoniot of shocked liquid nitrogen. *Phys. Rev. B* **63**, 024203 (2000).
25. Mundy, C. J. *et al.* Ultrafast transformation of graphite into diamond: an *ab initio* study of graphite under shock compression. *J. Chem. Phys.* **128**, 184701 (2008).
26. Goncharov, A. F. *et al.* Dynamic ionization of water under extreme conditions. *Phys. Rev. Lett.* **94**, 125508 (2005).
27. Schwegler, E., Sharma, M., Gygi, F. & Galli, G. Melting of ice under pressure. *Proc. Natl Acad. Sci. USA* **105**, 14779–14783 (2008).
28. Goldman, N. *et al.* *Ab initio* simulation of the equation of state and kinetics of shocked water. *J. Chem. Phys.* **130**, 124517 (2009).
29. Reed, E. J., Manaa, M. R., Fried, L. E., Glaesemann, K. R. & Joannopoulos, J. D. A transient semimetallic layer in detonating nitromethane. *Nature Phys.* **4**, 72–76 (2008).
30. Reed, E. J., Fried, L. E. & Joannopoulos, J. D. A method for tractable dynamical studies of single and double shock compression. *Phys. Rev. Lett.* **90**, 235503 (2003).
31. Reed, E. J., Fried, L. E., Henshaw, W. D. & Tarver, C. M. Simulation technique for steady shock waves in materials with analytical equations of state. *Phys. Rev. E* **74**, 056706 (2006).
32. Reed, E. J., Maiti, A. & Fried, L. E. Anomalous sound propagation and slow kinetics in dynamically compressed amorphous carbon. *Phys. Rev. E* **81**, 016607 (2009).
33. Walsh, J. M. & Rice, M. H. Dynamic compression of liquids from measurements on strong shock waves. *J. Chem. Phys.* **26**, 815–823 (1957).
34. Mitchell, A. C. & Nellis, W. J. Equation of state and electrical conductivity of water and ammonia shocked to the 100 GPa (1 Mbar) pressure range. *J. Chem. Phys.* **76**, 6273–6281 (1982).
35. Shoemaker, E. M. in *The Physics and Astronomy of the Moon* (ed. Kopal, Z.) 283–359 (Academic Press, 1962).
36. Beer, E., Podolak, M. & Prialnik, D. The contribution of icy grains to the activity of comets I. Grain lifetime and distribution. *Icarus* **180**, 473–486 (2006).
37. Yano, K. & Horie, Y. Discrete-element modeling of shock compression of polycrystalline copper. *Phys. Rev. B* **59**, 13672–13680 (1999).
38. Goldman, N., Fried, L. E., Kuo, I.-F. W. & Mundy, C. J. Bonding in the superionic phase of water. *Phys. Rev. Lett.* **94**, 217801 (2005).
39. Goldman, N. & Fried, L. E. First principles simulation of a superionic phase of hydrogen fluoride (HF) at high pressures and temperatures. *J. Chem. Phys.* **125**, 044501 (2006).
40. Goldman, N. & Fried, L. E. X-ray scattering intensities of water at extreme conditions. *J. Chem. Phys.* **126**, 134505 (2007).
41. Geissler, P. L., Dellago, C. D., Chandler, D., Hutter, J. & Parrinello, M. Autoionization in liquid water. *Science* **291**, 2121–2124 (2001).
42. Wu, C., Fried, L. E., Yang, L. H., Goldman, N. & Bastea, S. Catalytic behaviour of dense hot water. *Nature Chem.* **1**, 57–62 (2009).
43. Bastea, S. & Fried, L. E. Exp6-polar thermodynamics of dense supercritical water. *J. Chem. Phys.* **128**, 174502 (2008).
44. Klamt, A. *COSMO-RS: From Quantum Chemistry to Fluid Phase Dynamics and Drug Design* (Elsevier, 2005).
45. Patterson, J. E., Dreger, Z. A., Miao, M. & Gupta, Y. M. Shock wave induced decomposition of RDX: time-resolved spectroscopy. *J. Phys. Chem. A* **112**, 7374–7382 (2008).
46. VandeVondele, J. *et al.* Quickstep: fast and accurate density functional calculations using a mixed Gaussian and plane waves approach. *Comp. Phys. Comm.* **167**, 103–128 (2005).
47. Goedecker, S., Teter, M. & Hutter, J. Separable dual-space gaussian pseudopotentials. *Phys. Rev. B* **54**, 1703–1710 (1996).
48. Becke, A. D. Density-functional exchange-energy approximation with correct asymptotic behavior. *Phys. Rev. A* **38**, 3098–3100 (1988).
49. Lee, C., Yang, W. & Parr, R. G. Development of the Colle–Salvetti correlation-energy formula into a functional of the density. *Phys. Rev. B* **37**, 785–789 (1988).
50. Zel'dovitch, Y. B. & Raizer, Y. P. *Physics of Shock Waves and High-Temperature Hydrodynamic Phenomena* (Dover Publications, 2002).

Acknowledgements

This work was performed under the auspices of the US Department of Energy by Lawrence Livermore National Laboratory (LLNL) under Contract DE-AC52-07NA27344. The project 06-ERD-037 was funded by the Laboratory Directed Research and Development Program at LLNL. Computations were performed at LLNL using the massively parallel computers Thunder, ATLAS, uP, UM, UV, Gauss and Prism. We acknowledge L. Krauss for help with constructing the graphics in Figs 2 and 4.

Author contributions

N.G. originated the central idea for this work and performed and analysed the simulations. E.J.R. is lead author for the MSST algorithm and helped write the paper. L.E.F. co-created the MSST algorithm, wrote the molecular analyser code and helped write this paper. I.W.K. helped with the initial equilibration simulations. A.M. performed the Gibbs free energy of reaction calculations.

Additional information

The authors declare no competing financial interests. Supplementary information accompanies this paper at www.nature.com/naturechemistry. Reprints and permission information is available online at <http://ngp.nature.com/reprintsandpermissions/>. Correspondence and requests for materials should be addressed to N.G.